

PARTICLE PROPAGATION, WAVE GROWTH AND ENERGY DISSIPATION IN A FLARING FLUX TUBE

S. M. White,* D. B. Melrose** and G. A. Dulk***

*Astronomy Program, University of Maryland, College Park, MD 20742, U.S.A.

**Department of Theoretical Physics, University of Sydney, N.S.W. 2006, Australia

***Department of Astrophysical, Planetary and Atmospheric Sciences, University of Colorado, Boulder, CO, U.S.A.

ABSTRACT

We investigate wave amplification by downgoing particles in a common flare model. The flare is assumed to occur at the top of a coronal magnetic flux loop, and results in the heating of plasma in the flaring region. The hot electrons propagate down the legs of the flux tube towards increasing magnetic field. It is simple to demonstrate that the velocity distributions which result in this model are unstable to both beam instabilities and cyclotron maser action. We present an explanation for the propagation effects on the distribution, and explore the properties of the resulting amplified waves. We concentrate on cyclotron maser action, which has properties (emission in the z mode below the local gyrofrequency) quite different from maser action by other distributions considered in the context of solar flares. The z mode waves will be damped in the coronal plasma surrounding the flaring flux tube, and lead to heating there. This process may be important in the overall energy budget of the flare. We compare the downgoing maser with the loss cone maser, which is more likely to produce observable bursts.

INTRODUCTION

The observations of millisecond microwave bursts from the sun (e.g., /1/) strongly suggests the presence of maser action in the solar corona. This has led to interest in the possibility of electron cyclotron maser action in solar flares, resulting from various model distribution functions /2,3,4,5,6/. Rather than arbitrarily choose a distribution function, here we take a common flare model in which plasma at the top of a magnetic flux loop in the corona is heated, and show that, in addition to beam instabilities, electron cyclotron maser action should naturally occur in particles travelling down the legs of the flux loop (a result which has not previously been demonstrated). The characteristics of the resulting radiation are quite different from previously considered cases, and we compare them with the more familiar loss cone maser /2,3/.

VELOCITY DISTRIBUTIONS

Our basic model consists of a magnetic flux loop (Figure 1). Let z be the distance measured along a magnetic field line away from the top of the loop. The magnetic field in the loop is taken to be of the form $B(z) = B_0(1 + z^2/d^2)$, i.e., increases towards the feet of the loop with a characteristic scale height d . We suppose that a region of length L at the top of the loop is suddenly heated by the flare energy release. The case of a steady release of hot plasma produces essentially identical results for the maser emission by downgoing particles. We investigate the case when the velocity distribution of the heated plasma is Maxwellian and isotropic, which is implied by the thermal interpretation of impulsive hard X-ray and microwave bursts /7/. As we show below the important features of the distributions are not model dependent, and the model may be easily modified to include other initial velocity distributions /8/.

The heated particles have Coulomb mean free paths longer than a typical flux loop and stream down the legs away from the heated region. We look at the velocity distribution of hot electrons at a height z in a leg as a function of time. Liouville's equation may be solved for the velocity distribution given the above model. We find /9/ the evolution shown in Figure 2, where the velocity distribution is plotted as a contour diagram in $v_z - v$ space for four different times at the same height, where v_z and

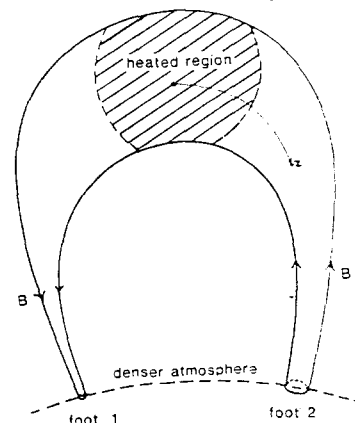


Fig. 1. The geometry of a coronal magnetic flux loop.

v_{\parallel} are the velocity components parallel and perpendicular to \mathbf{B} respectively. At early times ($z/t \gg v_T$) the distribution looks like a beam (Figure 2a). However at later times the distribution resembles a ring segment.

The basic physics which produces a distribution of this type is easily understood. Conservation of v_{\parallel} and of magnetic moment means that in velocity space (v_{\parallel} - v_{\perp}) particles move towards greater v_{\perp} on circles of constant radius as they travel down the field lines. Particles arriving at a given height at the same time all tend to start with the same v_z , and the change in pitch angle produces the ring shape. These features depend only on the assumption that the energetic particles come from localized heating and propagate towards increasing magnetic field strength. Distributions with this ring-segment feature have been seen in the earth's auroral zones /10/.

Beams radiate electrostatic waves by the well-known bump-in-the-tail instability. The fastest growing mode is the "slow plasma wave" at $\omega = \omega_p$ (assuming that $\omega_p < \Omega$ in the flaring region). Here we concentrate on the ring segment distributions. The next section discusses the basic features of cyclotron maser theory, and in the following section we use the results to deduce the properties of radiation by the ring-segment distributions.

A QUICK GUIDE TO CYCLOTRON MASER THEORY

In a cyclotron maser /11/ the energy inversion is provided by a positive gradient in the perpendicular velocity component. All particles which satisfy the condition

$$\omega - s\Omega/\gamma - k_z v_z = 0 \quad (1)$$

contribute to the growth or damping of a wave with frequency ω and parallel wavenumber k_z , where s is the harmonic number, Ω the gyrofrequency and γ the Lorentz factor. The solution of (1) is an ellipse in v_z - v_{\perp} space. The ellipse (e.g. Figure 3) has a centre at $v_z = v_0$, a semi-major axis length \tilde{V} parallel to the v_{\perp} -axis, and an eccentricity e , which depend on the ratios $s\Omega/\omega$ and $k_z c/\omega$. When $\omega > s\Omega$, $v_0 > V$; when $\omega < s\Omega$, $v_0 < V$; and e is small when $k_z c/\omega$ is small. The maser amplifies a wave (ω, k_z) if $\partial f/\partial v_{\perp} > 0$ overall on the ellipse defined by (1). Here we concentrate on the limit $\omega \ll \Omega$ which is likely to apply to solar flares. The wave modes which a cyclotron maser can amplify are the following magnetoionic modes (n is the refractive index):

$$\begin{array}{ll} \text{x mode, } \omega > \omega_x = \Omega + \omega_p^2/\Omega, & n < 1, \text{ RH polarised} \\ \text{o mode, } \omega > \omega_o, & n < 1, \text{ LH polarised} \\ \text{z mode, } \omega_p < \omega < \omega_{UH} = \Omega + 1/2 \omega_p^2/\Omega, & n > 1, \text{ RH polarised.} \end{array}$$

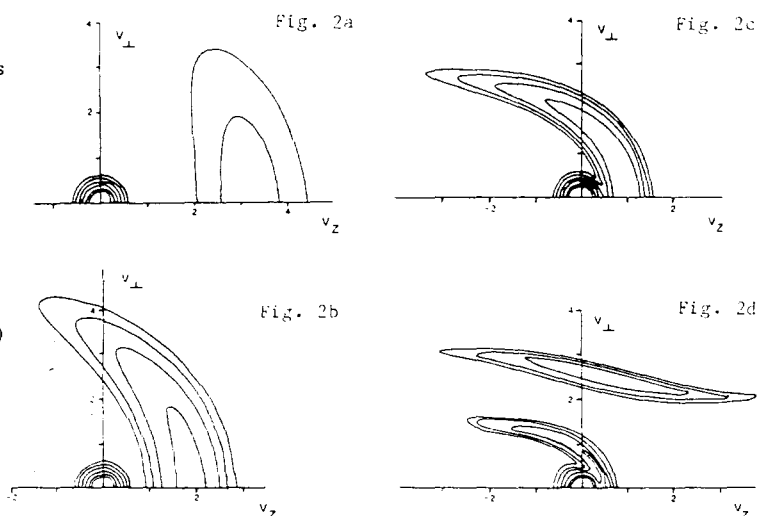
Since electron gyration corresponds to RH polarization the x or z mode will be favored.

MASER EMISSION BY DOWNGOING PARTICLES

To find the waves with the fastest growth rates we simply choose the ellipse which passes through regions where $\partial f/\partial v_{\perp}$ is largest. Such an ellipse (A) is shown for the ring-segment distribution of Figure 3. It has the following properties: $V \gg v_0$, $e \ll 1$. These conditions imply that $|n \cos \theta| \ll 1$, where θ is the angle between \mathbf{k} and \mathbf{B} , and

$$\frac{\omega^2}{s^2 \Omega^2} < 1 - n^2 \cos^2 \theta. \quad (2)$$

Fig. 2. The velocity distribution (presented as a contour plot in v_z - v_{\perp} space) as a function of time at the height $z=2d$, after a region of dimension $L=0.25d$ at the top of the flux loop ($z=0$) is heated from 10^6K to 10^8K at $t=0$. The four plots are at the following times: (a) $t=0.5d/v_T$; (b) $t=d/v_T$; (c) $t=2d/v_T$; (d) $t=4d/v_T$, where v_T is the thermal speed of the hot particles. Downgoing particles are on the right-hand-side of the figures, while upgoing particles are on the left-hand-side.



Thus (2) implies that wave amplification is largest at frequencies $\omega < s\Omega$, i.e., just below harmonics of the gyrofrequency. Emission at the fundamental is in the z mode (the only RH polarized mode at $\omega < \Omega$), and emission at $s = 2$ is in the x mode. The second ellipse (B) shown on Figure 3 will give smaller temporal growth rates. This may be important for the following reason. Ellipse B has $v_0 > V$, and allows growth at $\omega > \Omega$. In particular, for $\omega_p \ll \Omega$, waves may grow at $\omega = \omega_+(\theta) = \Omega + \frac{1}{2}\omega_p^2 \sin^2 \theta / \Omega$, where the group velocity is very small, so that these waves can have a large spatial growth rate. If wave growth is spatially limited this may be important.

Figure 4 shows the results of numerical calculations of the maximum temporal growth rate of the different modes as a function of the plasma parameter ω_p / Ω . The distribution used for this calculation is described by the parameters $z/d = 2$, $v_{Te}/d = 2$ and $L/d = 0.25$, where v_T is the thermal speed of the hot electrons. The temperature of the plasma heated at the top of the flux loop was taken to be 10^8 K, and the effects of a cool ambient plasma at 10^6 K are included (for this calculation the hot plasma density is diluted relative to the cooler ambient plasma by a factor of .01). Note that due to plasma effects the z mode is no longer the fastest growing mode for the larger values of ω_p / Ω . The x mode just below $\omega = 2\Omega$ then has a faster growth rate. There are several free parameters in this model, and the value of ω_p / Ω at which the second-harmonic x mode becomes the fastest growing mode varies depending on the choice of z and t . However the relative growth rates of the different modes shown in Fig. 4 depend only on the basic shape of the ring-segment velocity distribution, and hence are largely independent of the free parameters.

DISCUSSION

- (i) The full implications of maser action in this model are discussed elsewhere /8/. Briefly, a significant fraction of the energy of the heated particles may be radiated as waves while the particles are downgoing, at a phase of the flare before the loss cone maser has had time to develop. Saturation of wave growth is by wave-particle scattering.
- (ii) Often the electrostatic and electromagnetic waves are amplified simultaneously by the same distribution function, and generally the electrostatic wave grows faster. Since the two waves are fed by different sources of free energy in the distribution, we argue that saturation of the electrostatic wave does not prevent growth of the electromagnetic wave. However, further work needs to be done on this question /13/.
- (iii) A related problem is the efficiency with which particle free energy is converted into waves. Analytic arguments suggest perhaps 30% efficiency, but numerical particle simulations always find wave saturation at lower values of 0.5 to 5% /13,14/. However, even 1% of the flare energy is a large amount of energy.
- (iv) The electromagnetic mode with the fastest temporal growth rate will be the z mode ($\omega < \Omega$) or the second harmonic x mode ($\omega < 2\Omega$), depending on the ratio ω_p / Ω . Wave energy in both these modes will be strongly damped in the harmonic layers, $\omega = \Omega$ for the z mode and $\omega = 2\Omega$ for the x mode. This leads to heating of these plasma layers.
- (v) The loss cone maser produces radiation at frequencies $\omega > s\Omega / 12$, i.e. at frequencies just above the harmonics of the gyrofrequency (principally the x mode) rather than just below as for the ring-segment maser. The layer heated by the ring-segment maser is closer to the flaring flux loop than the layer heated by the loss-cone maser (in the latter, fundamental x mode waves generated at $\omega = \Omega + \omega_p^2 / \Omega$ propagate to the $\omega = 2\Omega$ layer where they are damped). The heating may be responsible for the emission of the soft-X-ray plasma seen in flares (cf. /3/). In models where most of the flare energy is released by accelerating particles or heating plasma, maser radiation is the most efficient way of transporting energy across field lines. Such transport is necessary to explain soft-X-ray structures seen to be much larger than the flaring loops /15/.
- (vi) There are two ways in which maser action in downgoing particles can lead to observable bursts. Firstly, if amplification is spatially limited so that the z mode at $\omega > \Omega$ becomes intense, and if coalescence of two z mode waves to produce x and o mode waves at $\omega > 2\Omega$ is an efficient process, the resulting radiation may escape from the corona. Alternatively, if the parameter ω_p / Ω is large enough that the second harmonic x mode is the fastest growing mode, and if the propagating waves encounter the second-harmonic absorption layer inside the flaring flux tube where the velocity distributions are so perturbed that the waves are no longer damped, then they may escape and be observed /16/. It is likely that these conditions are only rarely satisfied; however, microwave spike bursts are a relatively rare phenomenon. By contrast, it is easier to envisage observable bursts produced by a loss cone maser since emission is then at frequencies just above the harmonics of Ω .

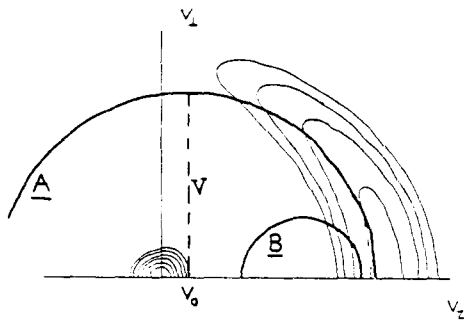


Fig. 3. Sketch of two types of ellipse, A and B, which pass through regions of positive $\partial f/\partial v$ for a ring segment distribution.

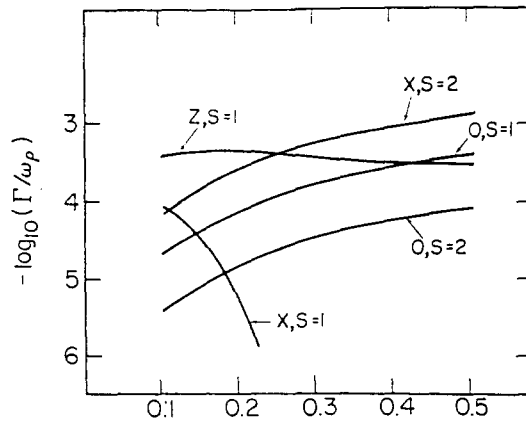


Fig. 4. The maximum growth rates of the magnetoionic modes as a function of ω_p/Ω for a ring segment distribution ($z = 2d$, $t = 2d/v_T$, $L = 0.25d$, $T_c = 10^6$ K, $T_h = 10^8$ K, $n_h = 0.01n_c$).

CONCLUSION

If a flare leads to localized heating of plasma in the corona, the hot particles propagating away from this region in the direction of increasing magnetic field naturally develop velocity distributions which are unstable to electron cyclotron maser action. The resulting maser has different characteristics from cyclotron masers previously considered in the solar context. About 10% of the hot-particle energy may be radiated as waves, and the main effect of these waves will be to heat coronal plasma in the vicinity of the flaring flux loop.

Part of this work was supported by NASA grants NAGW-91 and NSG-7287.

REFERENCES

1. C. Slottje, 1978, *Nature* 275, 520.
2. D.B. Melrose and G.A. Dulk, 1982, *Ap. J.* 259, 844.
3. D.B. Melrose and G.A. Dulk, 1984, *Ap. J.* 282, 308.
4. R.R. Sharma, L. Vlahos and K. Papadopoulos, 1982, *Astr. Ap.* 112, 377.
5. H.P. Freund, and C.S. Wu, 1984, *Radio Sci.* 19, 519.
6. R.M. Winglee, 1985, *Ap. J.* 291, 160.
7. C.J. Crannell, K.J. Frost, C. Matzler, K. Ohki and J.L. Saba, 1978, *Ap. J.* 223, 620.
8. S.M. White, D.B. Melrose and G.A. Dulk, 1986, *Ap. J.*, in press.
9. S.M. White, D.B. Melrose and G.A. Dulk, 1983, *Proc. ASA* 5, 188.
10. N. Omid, C.S. Wu and D.A. Gurnett, 1984, *J. Geophys. Res.* 89, 883.
11. C.S. Wu and L.C. Lee, 1979, *Ap. J.* 230, 621.
12. D.B. Melrose, R.G. Hewitt and G.A. Dulk, 1984, *J. Geophys. Res.* 89, 897.
13. R.M. Winglee and P.L. Pritchett, 1986, in preparation.
14. P.L. Pritchett, 1984, *J. Geophys. Res.* 89, 8957.
15. A. Duijveman, P. Hoyng and M. Machado, 1982, *Solar Phys.* 81, 137.
16. L. Vlahos, R.R. Sharma and K. Papadopoulos, 1983, *Ap. J.* 275, 374.